DOI: 10.26418/positron.v13i2.61621

Characteristics of Internal Solitary Waves near Its Generation Site in the Lombok Strait, Indonesia

Adi Purwandana[a*], Edikusmanto[a], Putri Adia Utari[a], Hilda Lestiana[b], Okta Fajar Saputra[c], Qurnia Wulan Sari[d]

[a] Research Center for Oceanography, National Research and Innovation Agency (BRIN), Jl. Pasir Putih I Ancol Timur, Jakarta 14430, Indonesia
[b] Research Center for Geological Resources, National Research and Innovation Agency (BRIN), Jl. Sangkuriang Bandung 40135, Indonesia
[c] Research Center for Geospatial, National Research and Innovation Agency (BRIN), Cibinong Science Center, Jl. Raya Jakarta-Bogor Km. 46, Bogor 16911, Indonesia
[d] Faculty of Fisheries and Marine Sciences, Padjadjaran University, Sumedang, 45363, Indonesia
*Email: adip003@brin.go.id
(Received 24 January 2023; Revised 24 May 2023; Accepted 27 May 2023; Published 31 November 2023)

Abstract

Evidence of internal solitary waves (ISWs) formation through the Lee wave mechanism in the Lombok Strait was revealed from the echosounder measurements conducted in November 2017. This study is aimed to characterize the property of ISW packet formed around ~30 km away from the generation site, in the southern part of the strait above the Nusa Penida Sill (NPS), by employing Korteweg-de Vries (KdV) solution. The packet can be categorized as the early stage of ISW formation, consisting of two waves of depression, with typical amplitude of 30 m and 10 m, for the first and second wave, respectively. The waves propagated northward with a typical phase speed of ~1.2 m·s^{-1}. The waves drive a maximum horizontal velocity anomaly of ~0.8 m·s^{-1} and a vertical velocity anomaly of ~10 cm·s^{-1}. The amplitude of the ISW packet will be potentially amplified during their propagation away from the strait. This study provides an observational based understanding on the early stage of internal tides evolution in the Lombok Strait, particularly highlights the energy transfer of internal tides through the propagation of internal solitary waves.

Keywords: soliton, Indonesian seas, KdV equation, single beam echosounder

1. Backgrounds

The Indonesian seas are featured by complex topography and strong barotropic tidal currents where their interaction drives strong internal tide generation, which can later evolve into internal solitary waves (ISWs) [1–5]. Formed due to internal tide evolution, the ISW is the only mechanism to transport internal tide energy away from their generation site.

There are two main mechanisms of ISW formation. Firstly it can be formed through nonlinear steepening processes [6], and secondly, due to the slackening of lee waves under supercritical conditions [7]. Practically, these mechanisms can be evaluated by inspecting the ratio between the maximum barotropic velocity and the mode-1 velocity, the *Froude number* (*Fr*). The flow gets supercritical if *Fr* close to unity; hence the ISW formation will be categorized due to lee wave mechanisms [8]. ISW can also be formed due to the collision of two water masses with a strong density gradient, occurring mainly in estuarine waters [9]. Characterization of ISW in the Indonesian seas has been performed since last decade, taking benefit of their frequent appearance in satellite imagery [10–14]. Note that ISW is manifested as a rough-slicky pattern on the sea surface as the region of convergence and divergence due to surface horizontal currents associated with these waves can modify the surface roughness. Previous studies successfully characterized the waves horizontally, including their propagation/phase speed. The concern about the wave characteristics vertically increased after the tragedy of the sunken Indonesian Naval Submarine, the Nanggala 402, on 21 April 2021, which was possibly triggered by ISW activity in the northern Bali waters. Recent studies have characterized the ISW vertically using satellite imagery [15,16] and numerical modeling [1,17].

The ability of the waves to transport remotely

the internal tide energy benefits local ecosystems once the waves break on the shore. Despite giving important mechanisms which support productivity due to nutrient enrichment for the pelagic system [18,19], the wave breaking may potentially harm the coastal environment due to pollutant resuspension in the sediments [20].

This study aims to tackle the knowledge gap related to ISW characteristics in the Lombok Strait, particularly in the location close to the generation site, by quantifying the intrinsic parameters of the ISW packet, including its energetic aspects, in its early stage of formation.

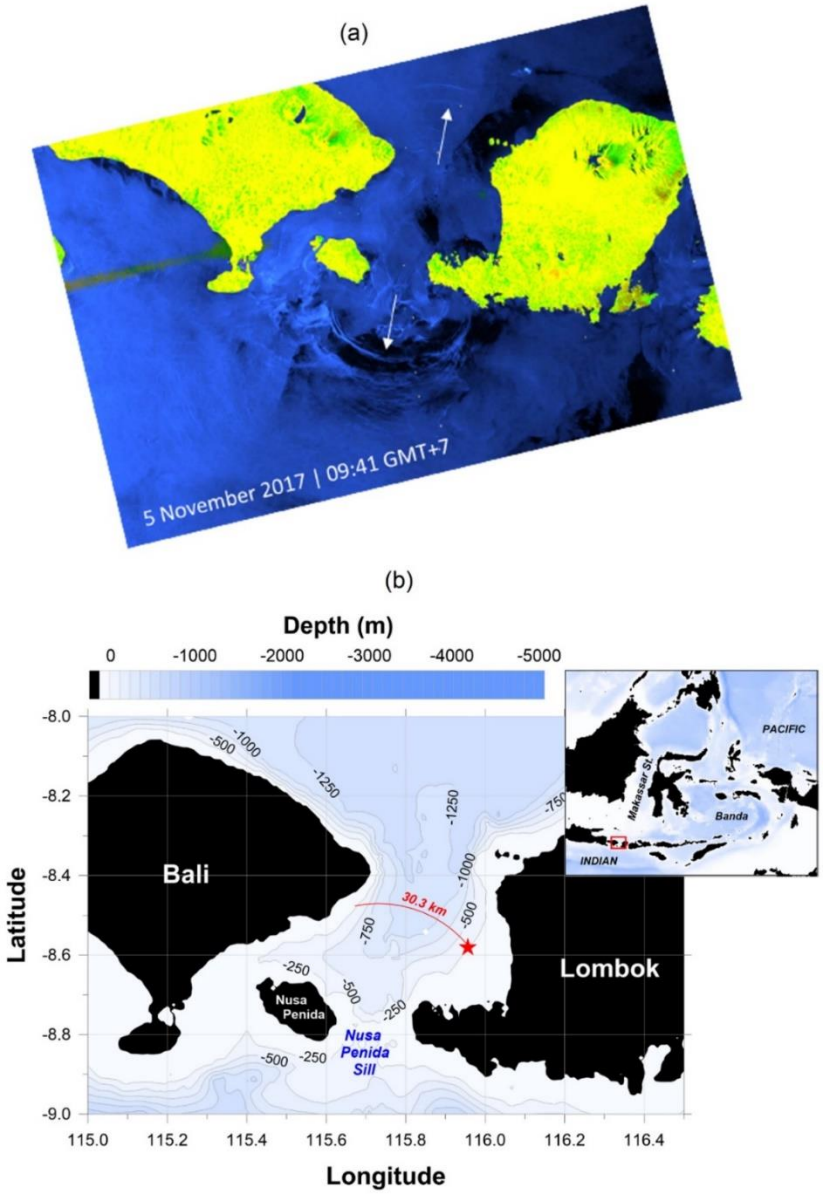

Figure 1 (a) The appearance of two packets of internal solitary waves (ISWs, white arrows) propagating northward and southward in the Synthetic Aperture Radar (SAR) images on 5 November 2017 (https://search.asf.alaska.edu) at 09.41 GMT+7 or around a day after the field observation. (b) Map of Lombok Strait waters with topography inferred from ETOPO. The location of observation on 4 November 2017 is presented in a red star. The datasets consisted of direct *Simrad* echosounder EK80 from 03.00 – 07.00 GMT+7 and single CTD measurements at 02.10 GMT+7, and from HYCOM product at 00.00 GMT+7. The red curve represents the sketch of the horizontal extent of the solitary wave (30.3 km) used to estimate the tidal energy flux.

2. Methodology

Four hours length of the Simrad single beam echosounder EK80 datasets was screened and analyzed in this study. Using the anchored boat method, the echosounder recorded the echo scattering layer at 200 kHz at ~8 km offshore the Mataram City of Lombok Island (116.02° E, 8.56° S). The measurement was conducted on 4 November 2017 during the early stage of the spring tide period. The maximum topography depth of the location is 250 m. Vertically, the echosounder covered up to 150 m yet can still capture the appearance of the ISW event since the interface between the surface mixed layer and the thermocline layer was located at ~50 m depth. Note that the maximum amplitude of the mode-1 ISW occurred in the upper thermocline layer. Figure 1a shows the location of observation.

The CTD (conductivity-temperature-depth) probe was also deployed to supply the water masses properties needed for the ISW analysis, casted around 1 hour before the passage of the ISWs (4 November 2017 at 02.12 GMT+7). Since the CTD cast was only lowered down to 200 m depth and the

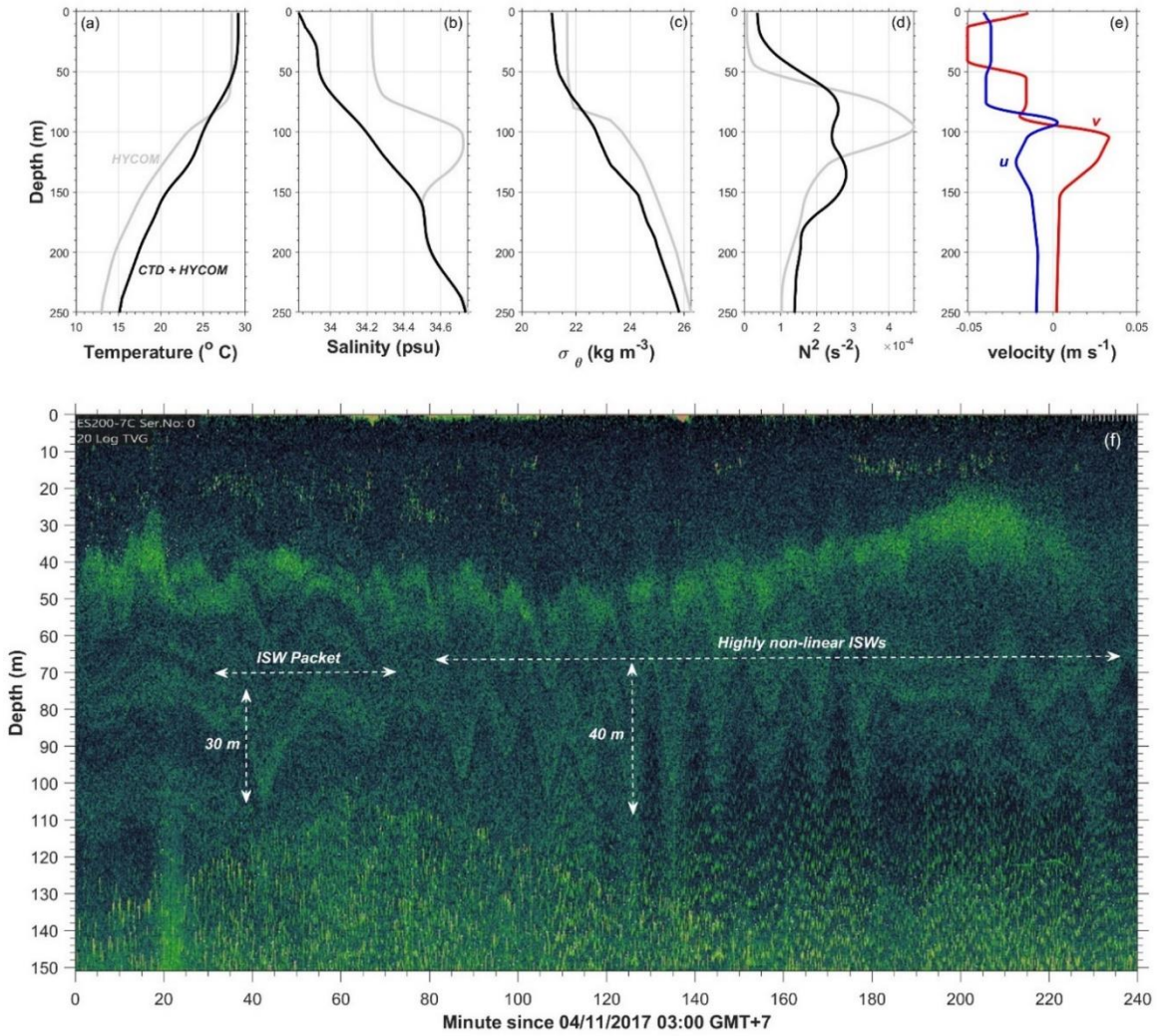

Figure 2 (a – e) the vertical profiles of potential temperature, salinity, density anomaly, stratification (represented by squared buoyancy frequency), and velocity components, respectively. The HYCOM profile is plotted in gray lines and the profile which considered both HYCOM and CTD observation (used in this study) is plotted in black lines. (f) The existence of internal waves in 4 hours length echosounder image on 4 November 2017 since 03.00 GMT+7. Two typical waves are also indicated: ISW packet and highly nonlinear ISWs.

Table 1 The characteristics of the internal solitary waves (ISWs) in the Lombok Strait.

η_0 (m)	α (s^{-1})	β ($m^3 s^{-1}$)	C_p (m s^{-1})	Δ (m)	Max U (m s^{-1})	Max w (cm s^{-1})	Energy (MJ m^{-1})	
							APE	KE
30	-1.44×10^{-2}	2.73×10^{3}	1.22	275	0.78	10.27	4.97	5.72
10	-1.44×10^{-2}	2.73×10^{3}	1.13	476	0.24	1.82	1.18	0.90

current measurements by a portable Acoustic Doppler Current Profiler (ADCP) covered the depth range of 50 – 100 m only; we negotiated the temperature, salinity, and velocity profiles obtained from the hybrid coordinate ocean model (HYCOM) [21] to supply the full depth (250 m) of the temperature and salinity. The HYCOM datasets were acquired on 4 November 2017 at 00.00 GMT+7, 3 hours before the passage of the ISW packet; located at 116.00◦ E, 8.56◦ S. The salinity product from HYCOM overestimates the salinity from CTD observation in the thermocline layer, where the HYCOM strongly identified the maximum salinity of the North Pacific water mass yet the CTD observation detected almost less saline water mass. Therefore, we used the CTD from the observation for the upper 200 m and filled the remaining depth (200-250 m) with the HYCOM profile. The HYCOM and CTD observation discrepancy is mainly caused by local variabilities, such as the influence of fresher water mass from river discharge, that the hybrid datasets cannot resolve. Figure 2(a – d) shows the water mass properties, including the stratification profile.

The dataset of the echosounder contained the signatures of internal wave events (Figure 2.e). The analysis was focused on the packet of ISWs observed from around 30 – 80 minutes, the minutes since 4 November 2017 at 03.00 GMT+7. This packet consisted of two waves of depression, identified here as the leading (first) wave and the tailing (second) wave. The higher frequency waves observed after have been neglected in this study since they performed as highly nonlinear waves,

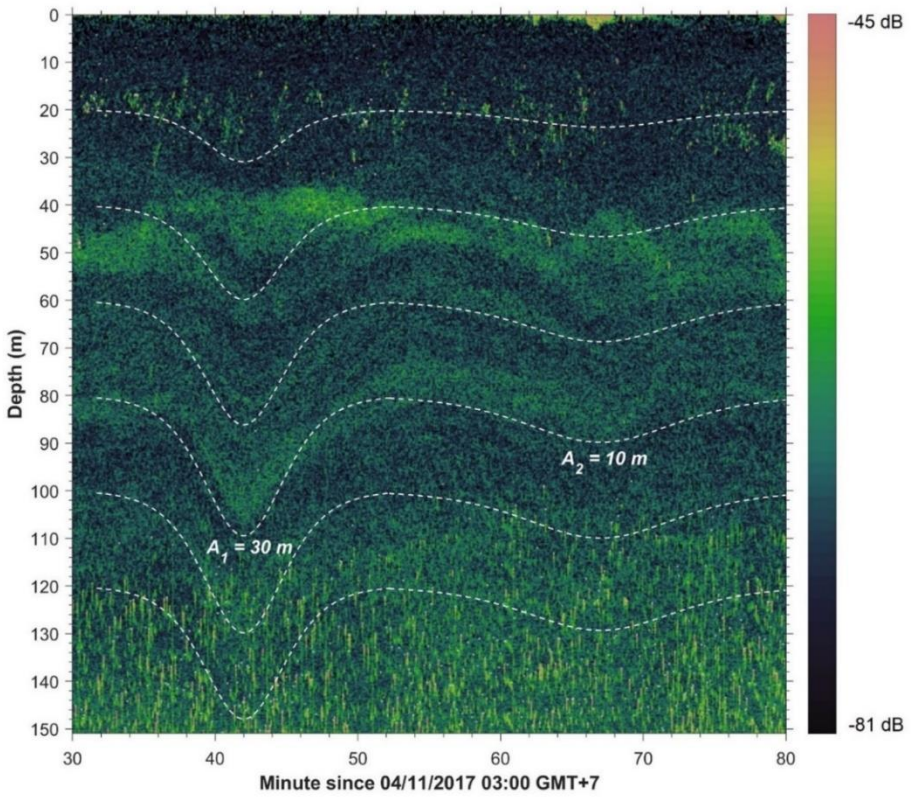

Figure 3 The time-basis plot of a packet of ISW with two ISWs. The fitting of the KdV (white dashed lines) at layer 20, 40, 60, 80, 100 and 120 m is overlaid on the echosounder image. The properties of the KdV fits refer to Table 1.

possibly due to the interaction with the side wall of the Lombok Strait, which may affect the nonlinearity of the waves [22]. Therefore, they cannot be considered the initial ISW packet stage emanating directly from the NPS.

A Korteweg-de Vries (KdV) solution is used to fit the sinusoid pattern of the wave that appeared in the echosounder. This method was also used recently to characterize ISW in the Indonesian seas [16,17]. The KdV is initially expressed as a balance between the nonlinearity (α) and dispersion (β) effects which stabilize the propagation (with a certain mode-1 velocity c_1) of the perturbed elevation $\eta(x,t)$ [16,23]:

$$\frac{\partial \eta}{\partial t} + c_1 \frac{\partial \eta}{\partial x} + \alpha\eta \frac{\partial \eta}{\partial x} + \beta \frac{\partial^3 \eta}{\partial^3 x} = 0 \qquad (1)$$

The solution of this equation follows a classical $sech^2$ form:

$$\eta = \eta_0 sech^2 \left[\frac{\left(c_1 + \frac{\alpha\eta_0}{3}\right)(t_0 - t)}{\Delta} \right] \qquad (2)$$

η_0 is the wave amplitude, the phase speed (Cp) term is expressed by (c_1+$\alpha\eta_0$/3), and the width of the wave can be estimated as $\Delta^2 = 12\beta/(\alpha\eta_0)$. The coefficients α and β are estimated as:

$$\alpha = \left(\frac{3}{2}\right) \frac{\int_{-H}^{0} (c_1 - U_b)^2 (d\Phi/dz)^3 dz}{\int_{-H}^{0} (c_1 - U_b)\,(d\Phi/dz)^2 dz} dz \qquad (3)$$

$$\beta = \left(\frac{1}{2}\right) \frac{\int_{-H}^{0} (c_1 - U_b)^2 \Phi^2 dz}{\int_{-H}^{0} (c_1 - U_b)\,(d\Phi/dz)^2 dz} dz \qquad (4)$$

Practically, η_0 is set initially by considering the wave height roughly estimated from the echosounder image pattern as the input for the KdV solution. $\Phi(z)$ is the vertical mode-1 structure of vertical displacement amplitude $\Phi(z)$, defined from the stratification profile $N^2(z)$. $\Phi(z)$ and the linear phase speed c_1 are solved using as [24]:

$$\frac{d}{dz}\left\{[c_1 - U_b(z)]^2 \frac{d\Phi}{dz}\right\} + N^2(z)\Phi = 0 \qquad (5)$$

with the boundary conditions $\Phi(-H) = \Phi(0) = 0$. Here, we considered only the meridional current component (v) of the HYCOM current profile as the background current profile $U_b(z)$ since the Lombok Strait has meridional relative mainstream. The result of this fitting method is shown in Error! Reference source not found..

To characterize the velocity profiles (w is the vertical current and U is the horizontal current) triggered by the wave, we calculate the 'pseudo' currents as [25]:

$$w = \frac{d\eta}{dt}\Phi \qquad (6)$$

$$U = C_p \frac{d\Phi}{dz} sech^2 \left[\frac{\left(c_1 + \frac{\alpha\eta_0}{3}\right)(t_0 - t)}{\Delta} \right] \qquad (7)$$

The energetic aspects of the wave are inspected by estimating the available potential energy (APE) and the kinetic energy (KE) as:

$$APE = \int_{-L}^{L} \int_{-H}^{0} \int_{0}^{h(z)} \rho(z) N^2(z') z' dz' dz dx \qquad (8)$$

$$KE = \frac{1}{2} \int_{H}^{0} \int_{-L}^{L} \rho(U^2 + w^2)\, dx dz \qquad (9)$$

with ρ(z) is the potential density.

3. Results and Discussions

As shown in Figure 2 (a – e), the hydrography of the Lombok Strait from the direct observation (CTD) is featured by fresher (< 34 psu) and warmer (~29°C) water mass compared to those from hybrid product (HYCOM) in the surface mixed layer; stratified current profile with strong southward current in the upper 100 m layer associated to the Indonesian throughflow (ITF), and reversed southward current below. The discrepancy between the HYCOM and CTD observation profiles, particularly on the appearance of maximum salinity in the thermocline layer related to the North Pacific thermocline water mass in the HYCOM profile, was not observed in the direct CTD measurements. The observation presented in this study was conducted during the late period of the Southeast Monsoon season. In the Lombok Strait, southward ITF is the major part controlling the current systems in the upper ~200 m layer (~ thermocline layer) and intrusion of northward flow below (see Hautala et al., 2001). The observation site was relatively close to the western coastal waters of Lombok Island. The discrepancy found between HYCOM and direct CTD observation, mainly in the upper layer, may occur because the HYCOM does not accommodate local variability, such as the presence of fresher water from the surrounding mainland, while the CTD observation does.

The ISW packet analyzed in this study consisted of two waves of depression, and they were successfully characterized using the KdV solution, which considered the background current. As shown in Figure 3, the best fit of the KdV results in a typical wave amplitude of 30 m and 10 m for the leading and trailing waves, respectively. The first wave was characterized by narrow width of ~275 m, and wider for the second wave of ~476 m. The waves propagated with a typical phase speed of 1.22 m s^{-1} and 1.13 m s^{-1} for the first and the second wave, respectively (see Table 1).

The waves triggered horizontal velocity (U) anomaly with a maximum value of ~0.8 m s^{-1} and maximum vertical velocity (w) anomaly of ~10 cm s^{-1}, which vertically extended to 190 m for isopleth 4 cm s^{-1}. Consisting of two waves only in the packet with a relatively moderate amplitude indicates that the packet was still in its early stage of propagation. As the waves propagate away from the generation site, the amplitude can grow, leading to splitting processes between the waves. This mechanism has also been indicated in modeling studies [5,17]. Horizontal and vertical current anomalies triggered by the waves are nearly half of the extreme solitary waves event (amplitude ~185 m, horizontal current ~2 m s^{-1}) observed during the East Indonesian Expedition of the Indonesian Institute of Sciences (LIPI).

The energetics aspect of the wave is evaluated based on the solitary waveform solution of the KdV equation. The APE and KE of the waves are presented in Table 1. The energy density of the first wave is APE = 4.97 MJ m^{-1} and KE = 5.72 MJ m^{-1}, where the total is two orders lower compared to the wave in the Maluku Sea [16] observed during the propagation stage. The vertical profile of the total energy density is shown in Figure 4.d.

The waves observed in this study contained less energy than the propagation stage of solitary waves observed in other regions, such as the South China Sea [27]. It is likely because the waves

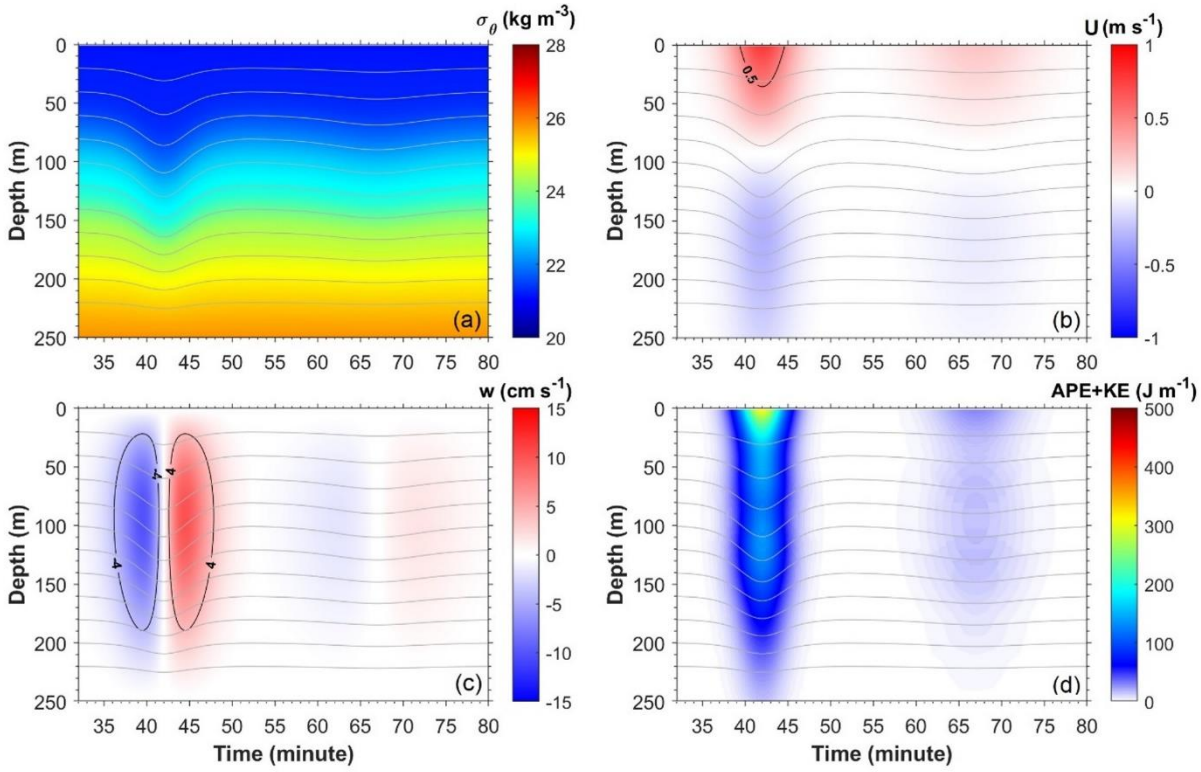

Figure 4 (a) Density perturbation during the passage of an ISW packet, (b) horizontal velocity (U – positive leftward), (c) vertical velocity (w – negative downward), and (d) total energy density ($KE+APE$). Gray lines represent the KdV fits at 20, 40, 60, 80, 100, 120, 140, 160, 180, 200, 220 m depth. The isopleth of 0.5 m s^{-1} and 4 cm s^{-1} is shown in (b) and (c), respectively. The properties of the KdV fits are shown in Table 1.

observed in this study were still in their early stage of formation. This less energy is also related to strong southward background current in the upper 100 m depth. To address this issue, a sensitivity test of the KdV solution to the background current was done for the leading wave of the packet. By omitting the background influence, the phase speed decreased by 11.4%; the width of the wave decreased by 13.4%; the APE and KE decreased by 16.4% and 23.1%, respectively; the horizontal and vertical velocity increased by 40.7% and 1.7%, respectively; and the internal tide energy flux decreased by ~20%. This test highlights the importance of including the background condition to characterize the ISW events. An assessment of the energetic aspect related to the mean energy flux per tidal cycle (12.41 h) with the arc front of ~30.3 km (red curve in Figure 1b) resulted in the mean energy flux per tidal cycle (12.41 h) of 10.1 MW was carried by the ISW packet northward. Further analysis cannot be done since the number of ISW packed released per tidal cycle; local internal tide energy dissipation was unclear due to limited datasets, and the location of the study is fairly close to the generation site.

The ISW packet was observed fairly close to their generation site in the NPS (~30 km), suggesting it was formed through the Lee wave mechanism. The waves analyzed in this study have a typical wave of depression; the mode-1 wave occurred in the waters where the ratio between the wave amplitude and depth of the water column is less than unity. Considering that the observation was conducted during the spring tide period over the NPS area [2], therefore the ISW packet presented here was produced due to the evolution of internal tide generated above the NPS.

4. Conclusions

This research provides the first observation-based study of an early-stage ISW packet formed in the Lombok Strait, located close to its generation site. This finding complements numerous satellite imagery which confirmed the northward propagating ISW packets inside the strait and can be used to validate future numerical modeling of ISW in the Lombok Strait. The sensitivity test related to the background currents presented in this study significantly reduce the phase speed, width of the wave, and total energy density, decreasing per tidal energy flux. The interaction between ISWs with the sloping topography of the Lombok and Bali shelves may increase the nonlinearity of the waves and induce strong mixing. Further comprehensive investigation and monitoring of ISW events, mainly in the Lombok Strait, is still needed to understand its behavior and extremity moments better since this passage is an international sea traffic lane and one of Indonesia's most crowded business centers of tourism. The presence of regular formation of ISW events should be well-informed to various parties.

5. Acknowledgment

All authors contributed equally as the main contributors. The author thanks the Indonesian Endowment Fund (LPDP) Kementerian Keuangan RI and *les Partenariats Hubert Curien* (PHC) Program by Campus France for funding this Project, Pak Asep from Ministry of Marine Affairs for helping the echosounder data acquisition, Dr. Yannis Cuypers and Pak Djatmiko Irianto for guiding the data acquisition, and Pak Hendra Munandar and Lombok Marine Station crew for facilitating the dormitory during the observation. This project is also supported by the research scheme of *Program Riset Unggulan* COREMAP CTI 2021 (17/A/DK/2021) and 2022 (4/III/HK/2022).

References

[1] Purwandana, A. , Cuypers, Y. , Bourgault, D. , Bouruet-Aubertot, P. , and Santoso, P. D. , Fate of internal solitary wave and enhanced mixing in Manado Bay, North Sulawesi, Indonesia, Continental Shelf Research, **245**(104801), 2022.

[2] Purwandana, A. , Cuypers, Y. , and Bouruet-Aubertot, P. , Observation of internal tides, nonlinear internal waves and mixing in the Lombok Strait, Indonesia, Continental Shelf Research, **216**2021.

[3] Robertson, R. and Ffield, A. , M2 Baroclinic Tides in the Indonesian Seas, Oceanography, **18**(4), pp.62–73, 2005.

[4] Nagai, T. and Hibiya, T. , Internal tides and associated vertical mixing in the Indonesian Archipelago, Journal of Geophysical Research: Oceans, **120**(5), pp.3373–3390, 2015.

[5] Aiki, H. , Matthews, J. P. , and Lamb, K. G. , Modeling and energetics of tidally generated wave trains in the Lombok Strait: Impact of the Indonesian Throughflow, Journal of Geophysical Research: Oceans, **116**(3), pp.1–

17, 2011.

[6] Gerkema, T. , A unified model for the generation and fission of internal tides in a rotating ocean, Journal of Marine Research, **54**(3), pp.421–450, 1996.

[7] Alford, M. H. , Peacock, T. , Mackinnon, J. A. , Nash, J. D. , Buijsman, M. C. , Centuroni, L. R. , Chao, S. Y. , Chang, M. H. , Farmer, D. M. , Fringer, O. B. , Fu, K. H. , Gallacher, P. C. , Graber, H. C. , Helfrich, K. R. , Jachec, S. M. , Jackson, C. R. , Klymak, J. M. , Ko, D. S. , Jan, S. , Johnston, T. M. S. , Legg, S. , Lee, I. H. , Lien, R. C. , Mercier, M. J. , Moum, J. N. , Musgrave, R. , Park, J. H. , Pickering, A. I. , Pinkel, R. , Rainville, L. , Ramp, S. R. , Rudnick, D. L. , Sarkar, S. , Scotti, A. , Simmons, H. L. , St Laurent, L. C. , Venayagamoorthy, S. K. , Wang, Y. H. , Wang, J. , Yang, Y. J. , Paluszkiewicz, T. , and Tang, T. Y. , The formation and fate of internal waves in the South China Sea, Nature, **521**(7550), pp.65–69, 2015.

[8] Maxworthy, T. , Note on the Internal Solitary Waves Produced By Tidal Flow Over a Three-Dimensional Ridge., J Geophys Res, **84**(C1), pp.338–346, 1979.

[9] Bourgault, D. , Galbraith, P. S. , and Chavanne, C. , Generation of internal solitary waves by frontally forced intrusions in geophysical flows, Nature Communications, **7**2016.

[10] Karang, I. W. G. A. , Nishio, F. , Mitnik, L. , and Osawa, T. , Spatial-Temporal Distribution and Characteristics of Internal Waves in the Lombok Strait Area Studied by Alos-Palsar Images, Earth Science Research, **1**(2), pp.11–22, 2012.

[11] Mitnik, L. , Alpers, W. , and Hock, L. , Thermal plumes and internal solitary waves generated in the Lombok strait studied by ERS SAR, European Space Agency, (Special Publication) ESA SP, (461), pp.1834–1842, 2000.

[12] Jackson, C. , Internal wave detection using the Moderate Resolution Imaging Spectroradiometer (MODIS), Journal of Geophysical Research, **112**(C11), pp.C11012, 2007.

[13] Chonnaniyah , Karang, I. W. G. A. , and Osawa, T. , Internal solitary waves propagation speed estimation in the northern-part of Lombok Strait observed by Sentinel-1 SAR and Himawari-8 images, IOP Conference Series: Earth and Environmental Science, **944**(1), 2021.

[14] Karang, I. W. G. A. , Chonnaniyah , and Osawa, T. , Internal solitary wave observations in the Flores Sea using the Himawari-8 geostationary satellite, International Journal of Remote Sensing, **41**(15), pp.5726–5742, 2020.

[15] Gong, Y. , Xie, J. , Xu, J. , Chen, Z. , He, Y. , and Cai, S. , Oceanic internal solitary waves at the Indonesian submarine wreckage site, Acta Oceanologica Sinica, **41**(1), pp.1–5, 2022.

[16] Purwandana, A. and Cuypers, Y. , Characteristics of internal solitary waves in the Maluku Sea , Indonesia, Oceanologia, (xxxx), 2022.

[17] Gong, Y. , Xie, J. , Xu, J. , Chen, Z. , He, Y. , and Cai, S. , Spatial asymmetry of nonlinear internal waves in the Lombok Strait, Progress in Oceanography, **202**pp.102759, 2022.

[18] Muacho, S. , Silva, J. C. B. Da , Brotas, V. , and Oliveira, P. B. , Effect of internal waves on near-surface chlorophyll concentration and primary production in the Nazaré Canyon (west of the Iberian Peninsula), Deep-Sea Research Part I: Oceanographic Research Papers, **81**pp.89–96, 2013.

[19] Muacho, S. , Silva, J. C. B. da , Brotas, V. , Oliveira, P. B. , and Magalhaes, J. M. , Chlorophyll enhancement in the central region of the Bay of Biscay as a result of internal tidal wave interaction, Journal of Marine Systems, **136**(1), pp.22–30, 2014.

[20] Gentil, M. , Floc'h, F. , Meunier, T. , Ruiz-Angulo, A. , Roudaut, G. , Perrot, Y. , and Lebourges-Dhaussy, A. , Internal solitary waves on the NW African shelf: A heuristic approach to localize diapycnal mixing hotspots, Continental Shelf Research, **226**(July), pp.104492, 2021.

[21] HYCOM, [Online]. Available: https://ncss.hycom.org/thredds/ncss/grid/GLBv0.08/expt_57.2/dataset.html. [Accessed: 05-Aug-2022]

[22] Zou, L. , Li, Y. , Hu, Y. , Wang, Z. , and Yu, Z. , Frontal collision of two nonlinear internal solitary waves in a stratified fluid, Applied Ocean Research, **104**(February), 2020.

[23] Ostrovsky, L. A. and Stepanyants, Y. A. , Do internal solitions exist in the ocean?, Reviews of Geophysics, **27**(3), pp.293–310, 1989.

[24] Shi, X. gang , Fan, Z. song , and Liu, H. long , A numerical calculation method for eigenvalue problems of nonlinear internal waves, Journal of Hydrodynamics, **21**(3), pp.373–378, 2009.

[25] Cai, S. , Xu, J. , Liu, J. , Chen, Z. , Xie, J. , Li, J. , and He, Y. , Retrieval of the maximum horizontal current speed induced by ocean internal solitary waves from low resolution time series mooring data based on the KdV theory, Ocean Engineering, **94**pp.88–93, 2015.

[26] Hautala, S. L. , Sprintall, J. , Potemra, J. T. , Chong, J. C. , Pandoe, W. , Bray, N. , and Ilahude,

A. G. , Velocity structure and transport of the Indonesian Throughflow in the major straits restricting flow into the Indian Ocean, Journal of Geophysical Research: Oceans, **106**(C9), pp.19527–19546, 2001.

[27] Klymak, J. M. , Pinkel, R. , Liu, C. T. , Liu, A. K. , and David, L. , Prototypical solitons in the South China Sea, Geophysical Research Letters, **33**(11), pp.5–8, 2006.